Study of immune cells' migration patterns in cancer

Author: Pau Canaleta Vicente
Facultat de Física, Universitat de Barcelona, Diagonal 645, 08028 Barcelona, Spain.

Advisor: Jordi Comelles Pujadas

Abstract: Immune cells' migration is a very important mechanism to respond to external infections or pathological process such as cancer. Although it is proved that cell migration in 3D spaces follow an anisotropic persistent random walk pattern (APRW), we prove in this work that this is not true for immune cells migrating in colorectal cancer ($APC^{-/-}$) conditioned media. We develop a segmentation model for 3D images in order to track the cells. With the trackings, we demonstrate that in this media immune cells migrate at higher velocity and with straighter paths, contrary to what is described by APRW model.
Keywords: Random walking, Image processing, Trajectory analysis, Subdiffusion
SDGs: SDG 3, SDG 15

I. INTRODUCTION

Cell migration is a process in which cells move in the medium in which they are located. It is a crucial mechanism for immune cells, as they have to be able to reach the place of the pathogenic threat. This directional migration typically are the response to environmental cues, such as chemical gradients, but in their absence migration could be seen as a random walk. Actually, cells migrating in 3 dimensions have been established to follow an anisotropic persistent random walk model (APRW model) [1], which is a particular case of random walking in which different persistent times and speeds are considered depending on the direction of the migration. However, it is not known whether immune cells exposed to pathological signals coming from cancer cells also behave as APR walkers.

To track cells moving in a three-dimensional space, it is necessary to use four-dimensional images, in which it is considered the position of coordinates x, y and z and the time. Taking good quality 4D images with low diffraction can be expensive, as high-quality confocal microscopes are a big investment. When simpler fluorescence microscopes are used, the images captured could be affected by diffraction, as out-of-focus light is not removed. This type of microscopes can use an algorithm to clear the image, but this processing is not enough to unequivocally detect cells present in the image. Thus, an additional filtering and segmentation algorithm should be implemented in order to correct those defects.

In this work, we will develop a segmentation model capable of detecting immune cells in four-dimensional images affected by diffraction. We have used colorectal cancer $APC^{-/-}$ organoids for defining the cancerous conditioned media and WT organoids for control. With the segmented images we will demonstrate that immune cells under the influence of cancerous conditioned media do not follow an APRW pattern (Fig. 1a).

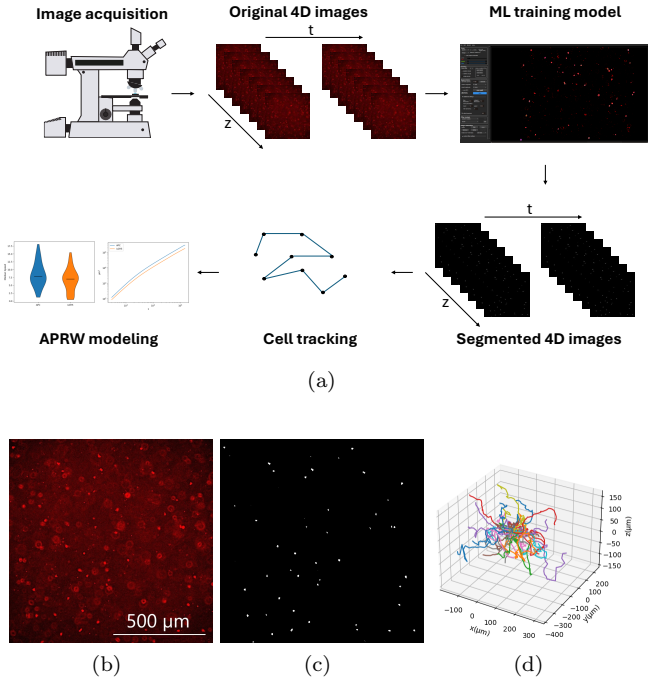

FIG. 1: (a) Procedure for modeling immune cells captured in four-dimensional images. (b) XY projection of a time frame from the original 4D image. (c) Segmentation of the previous image. (d) Origin-normalized 3D plots for tracks obtained in $APC^{-/-}$ conditioned media.

II. METHODS

A. Image acquisition

For the development of this project, we have analyzed 4D images (x, y, z, t) of immune cells moving in $APC^{-/-}$ conditioned media acting as the cancerous model and in WT conditioned media, which corresponds to control model. For each condition, two different 4D images were captured, each corresponding to a different repetition of

the experiment in the medium. The images were captured in IBEC facilities, in the laboratory of Dr. Elena Martínez (Biommimetics systems for cell engineering), with a Leica Thunder Imager Live Cell setup, using a x20 objective. Image z-stacks were acquired with a z-step of 5 μm and 5 minute intervals between z-stacks, resulting in a total time lapse of 6 hours.

B. Image segmentation

The images captured by the microscope presented diffraction effect that hindered the detection and tracking of the cells, as seen in Fig. 1b. In order to improve the quality of the images to be able to detect cells present in the capture, we had to segment them using Cellpose [2], a widely used software in biology for 2D and 3D image segmentation.

Images analyzed in Cellpose need to be preprocessed in order to reduce the effect of the diffraction and noise. To do so, we used Fiji image editor [3], which is used to open and edit 4D images obtained from different microscopy formats. We subtracted the maximum background possible using 'subtract background' function in Fiji and we adjusted the brightness and contrast to improve cell visualization. Cellpose algorithm is not capable of segmenting four-dimensional images; it supports a maximum of 3D. It is necessary to generate separate three-dimensional images for each time frame. Once the images are preprocessed, they are segmented using Cellpose algorithm. Pre-trained models included in Cellpose for image segmentation can be used, but not all the noise of the image will be removed and cells will not be well defined. To improve the segmentation process, we trained our own model using the Cellpose human-in-the-loop training system [4], where the user can intervene in the training process. With this system, the user can redefine the regions of interest (ROIs) that the program determined in the training process, correcting the mistakes made by the algorithm. This process accelerates the model training, and with just a few hours, Cellpose is able to define with reasonable precision the location and borders of the cells in 2D images.

To train a model for segmenting 3D images, it is necessary to have some samples of the orthogonal views. In this work, we used 4 images for each plane of the three-dimensional images, each of them showing significantly different regions of the image. With five human interventions after each training, the model was able to determine the cells in each image. Applying this model to each 3D image for each condition generates a set of 3D segmented images, which are saved assigning a different gray-level value to every ROI, while the lowest value is assigned to the background. It is necessary to re-stack the segmented images to 4D images in order to track the motion of the cells, as shown in Fig. 1a.

C. Cell tracking

Once the images are segmented, we defined the trajectories followed by immune cells using TrackMate software [5], a plugin for Fiji specialized in cell tracking. As it performs better for images where noise is very low, our data segmented with Cellpose should be suitable for the plugin.

As each segmented cell is assigned to a different gray-level value, TrackMate is able to identify each ROI present in the image, even if they are close together. We filtered the radius of the cells to remove minor errors from the segmentation process. To track cell migration, we used Linear Assignment Problem (LAP) [6]. This tracking method consists of linking the spots from one frame to another, considering the square distance from the previous position. It is possible to limit the maximum distance a cell can travel between time frames to have more accuracy in the trackings. The tracker favors linking between spots with similar features. This tracker also accepts gaps between frames in case some error has occurred in the segmentation process. An example of 3D tracks determined by TrackMate can be seen in Fig. 1d.

D. Trajectory analysis

To analyze the immune cell trajectories found by TrackMate, we used CellTracks Colab [7]. This script is able to determine the directionality, median speed, tortuosity and total turning angle of the tracks found. Directionality is defined as $D = \frac{d_{euclidean}}{d_{totalpath}}$, where $d_{euclidean} = \sqrt{(x_{end} - x_{start})^2 + (y_{end} - y_{start})^2 + (z_{end} - z_{start})^2}$ and $d_{totalpath}$ represents the total distance traveled. Directionality provides an insight into the straightness of the path, when the value is close to 1, the path is straighter. Tortuosity indicates the curvature and complexity of the track, and is defined as $T = \frac{d_{totalpath}}{d_{euclidean}}$. The total turning angle of the tracks is determined calculating the angle between to consecutive segments of a path. The sum of all values determine the total turning angle.

In this analysis, Cohen's d value is also determined. This value is used to determine the difference between two compared datasets. It is measured as $Cohen\ d = \frac{Condition\ A\ mean - Condition\ B\ mean}{Pooled\ standard\ deviation}$. As determined in [7], we can consider that the difference between two conditions is large when Cohen's d value is above 0.5.

E. Mean squared displacement

To analyze the tracks we also determine the mean squared displacement (MSD). MSD slope gives an indication of cell type of movement. For short time lags, cell predominant movement is diffusion, as it is the fastest movement at this scale. As time lag increases, three pos-

sible situations can occur. The first one is that the slope gets bigger, which indicates that cell movement is no longer diffusive and some other mechanism faster than diffusion is occurring (for example, ballistic movement). The second option is to not have any variation in the slope of MSD, which indicates that the movement continues to be diffusive. The third option is having a diminution of the slope, indicating the movement became subdiffusive. MSD is determined with the following equation:

$$MSD(\tau) = \langle \sum_{i=1}^{d} (x_i(t+\tau) - x_i(t))^2 \rangle, \quad (1)$$

where d depends on the number of dimensions.

F. PRW and APRW models

For adjusting both persistent random walk (PRW) and anisotropic persistent random walk (APRW) we used protocols described in [8], PRW and APRW models are fitted from the original tracks, finding persistence and speed values for each model. When the models are fitted, we simulate tracks using this parameters. With the simulated tracks, MSD is determined for comparison with the original tracks. To verify which model adjusts the best to original MSD values, we used root mean square error (RMSE), where lower values indicate lower difference between model and original values.

$$RMSE = \sqrt{\frac{1}{n} \sum_{i=1}^{n} (y_i - f_i)} \quad (2)$$

We also determined the autocorrelation function of cell velocities (ACF), which indicates if there is a correlation between past and present velocities. It is expected from this value to have high values at short time lags, but if there is no correlation between cell velocities, the value tends to 0 at longer time lags.

$$ACF(\tau) = \langle \sum_{i=1}^{d} \delta x_i(\tau) \delta x_i(t+\tau) \rangle, \quad (3)$$

III. RESULTS

A. Segmentation and tracking

We developed a segmentation model that was able to determine the position of the cells in each 3D time frame image. An example of a segmented XY plane can be seen in 1c. We obtained two four-dimensional segmented images for each condition. Segmented cells were tracked by TrackMate. Cells' track duration obtained vary from a few couple of time frames to the whole time lapse, because cells enter and leave the field of view during the experiments. In order to obtain a homogeneous dataset of tracks, we filtered the track duration, so the paths analyzed vary between two and a half hours and three and a half hours. An example of 3D origin-normalized tracks can be seen in 1d. Thus, we obtained four different three-dimensional tracks corresponding to a time lapse of 150-210 minutes, two sets tracks from $APC^{-/-}$ conditioned media and two sets from WT conditioned media.

B. Track analysis

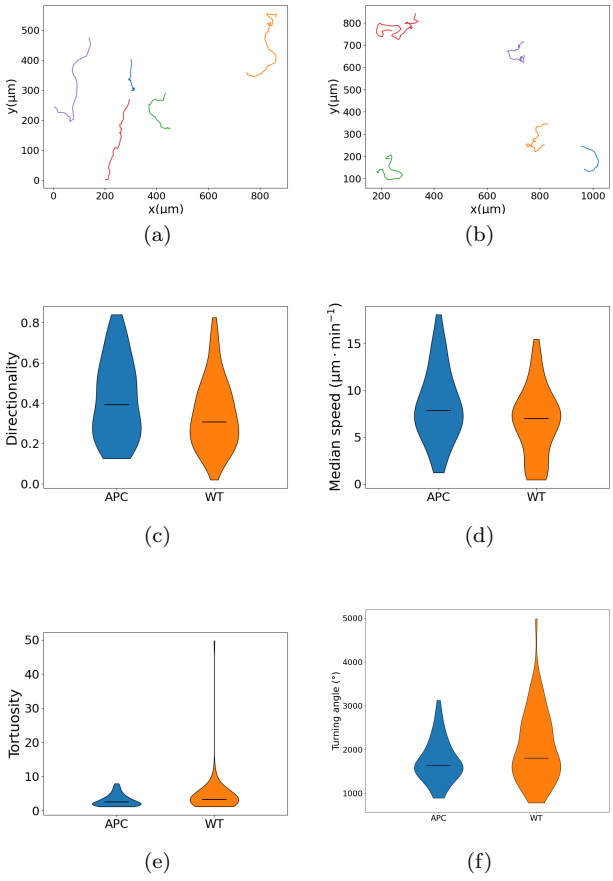

FIG. 2: 2D projection of 5 significant tracks of immune cells in $APC^{-/-}$ conditioned media (a) and in WT conditioned media (b). Violin graphs correspond to track comparison between cells in $APC^{-/-}$ media (blue) and WT media (orange). Median value of each graph is marked with black line. Directionality (c), Median speed (d), Tortuosity (e) and Turning angle (f). Cohen's d value for each parameter are: 0.41 (c), 0.52 (d), 0.29 (e) and 0.45 (f).

We first conducted the track analysis between repetitions of the experiments in same conditions in order to verify the repeatability of the data obtained. Comparing

both repetitions in WT media, we found small variation between them, obtaining Cohen's d values from 0.24 to 0.28. In $APC^{-/-}$ media, the variation between repetitions is higher than in control, obtaining Cohen's d values from 0.26 to 0.32. Although this values in cancerous media are higher, these differences are lower than 0.5, meaning the repetitions in both conditions are not large, so data can be merged for easier comparison.

Applying the same analysis to compare $APC^{-/-}$ and WT conditioned medias, we can see in Fig. 2c and Fig. 2d that directionality and median speed are higher in $APC^{-/-}$ conditioned media. We can also see in Fig. 2e and Fig. 2f that tortuosity and turning angle are slightly higher in WT conditioned media. Most notable difference is found in velocity, where Cohen's d value is 0.52. We can observe that the maximum velocity is higher in cells present in $APC^{-/-}$ conditioned media. Comparing the maximum velocity between each condition, we find a Cohen's d value of 0.62, meaning cells in $APC^{-/-}$ move at higher velocities. Thus, immune cells migrating in WT media present slightly higher tortuosity and total turning angles and migration in $APC^{-/-}$ conditioned media is faster and more directional.

C. Immune cells follow an APRW model in control conditions

We calculated MSD for each set of tracks in order to verify that immune cells migrating in WT conditioned media follow an APRW model. As we can see in Fig. 3e, MSD from simulated PRW and APRW models are compatible with original MSD and their error bars. The error bars in Fig. 3e and 3f correspond to the standard error of the mean, calculated using the following expression,

$$\sigma = \sqrt{\frac{\sum_{i=1}^{n}(x_i - \bar{x})^2}{n}} \tag{4}$$

where x_i corresponds to the value of MSD in a repetition and $\bar{x}$ corresponds to MSD when both condition repetitions tracks are unified. In Tab. I we calculated RMSE as defined in 3. The RMSE value in APRW model is lower than in PRW model, meaning APRW is a better adjustment to the tracks. We can also see that the slope of the MSD decreases with higher time lag values, indicating the predominant movement is subdiffusive, as predicted by random walk models. Thereby, we demonstrate that immune cells migrating in WT conditioned media follow an APRW model.

D. Immune cells under $APC^{-/-}$ conditioned media do not migrate as APR walkers

In Fig. 3e we can see that both PRW and APRW models fail to predict the behavior of immune cells migrating in $APC^{-/-}$ conditioned media. In short time lags, behavior is diffusive as predicted, but as the time lag becomes bigger, predicted models decrease the slope acquiring a subdiffusive motion where original immune cells continue to move with lineal diffusive motion ($R^2 =$

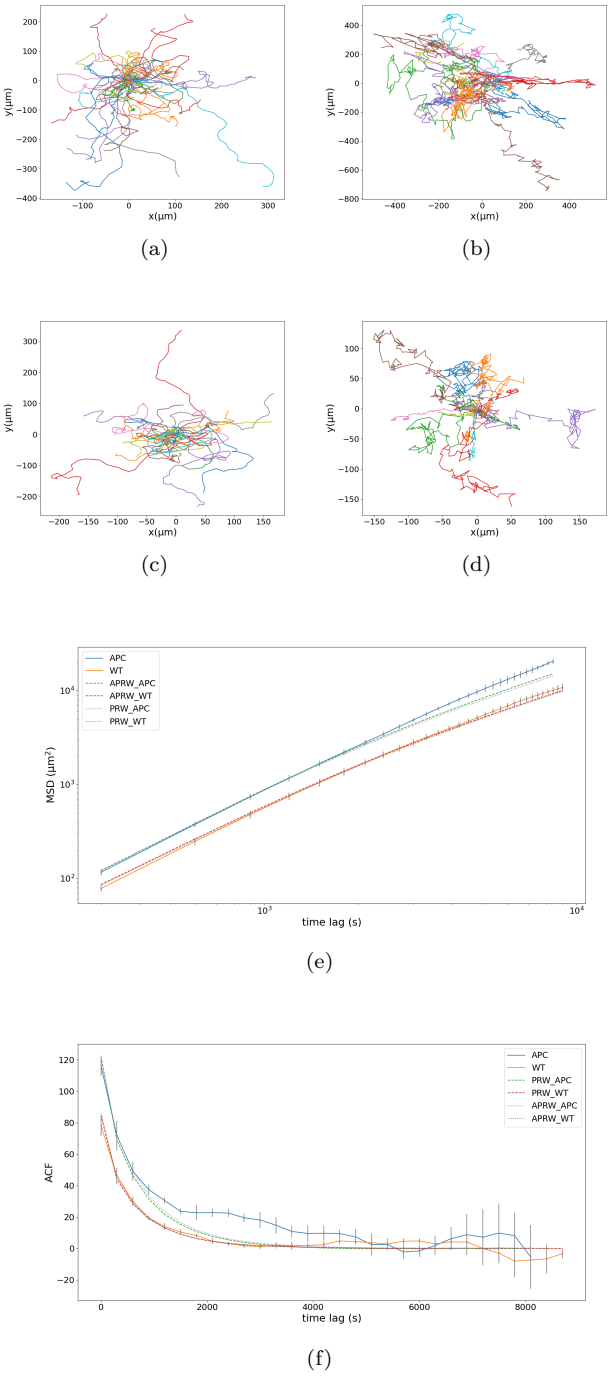

FIG. 3: First 4 images correspond to the origin-normalized 2D projection of the 3D tracks. (a) Original $APC^{-/-}$ tracks. (b) Simulated $APC^{-/-}$ tracks as APR walkers. (c) Original WT tracks. (d) Simulated WT tracks as APR walkers. Representation of the calculated MSD (e) and ACF (f) values for each original and simulated tracks.

Condition	RMSE (MSD)	RMSE (ACF)
APRW WT	320.29	0.22
PRW WT	426.21	0.38
APRW APC	1848.95	6.19
PRW APC	2190.40	6.95

TABLE I: Calculated RMSE of MSD and ACF values corresponding to each condition.

0.99). In Tab. I it is shown that APRW model is a better approximation to real behavior. Thus, we demonstrate that although APRW is a better approximation than PRW, both models fail to predict migration patterns in $APC^{-/-}$ conditioned media.

E. Migration in $APC^{-/-}$ conditioned media is faster than in WT media

As stated before in this work, analysis made by CellTracks Colab determined that migration velocities in $APC^{-/-}$ conditioned media are higher that in WT media. To verify this statement, we will determine the diffusion coefficients for both conditions. We can calculate the coefficients from MSD with the following equation, $MSD = 2dD\tau$, where d corresponds to the number of dimensions, and D to the diffusion coefficient. In the WT conditioned media we find a diffusive coefficient of $D = 0.15 \pm 0.01\mu^2 s^{-1}$. In $APC^{-/-}$ conditioned media, we find $D = 0.43 \pm 0.01\mu^2 s^{-1}$. Therefore, diffusion coefficient in $APC^{-/-}$ is significantly higher than in WT media, indicating higher velocities in $APC^{-/-}$ conditioned media, as determined previously.

F. Immune cell velocities are not correlated

In Fig. 3f we have determined and represented the ACF values for the original tracks and the simulated ones. For WT conditioned media we can observe that original and simulated tracks follow the same pattern and the ACF tends to zero with time. In $APC^{-/-}$ conditioned media we can also observe this behavior, although some correlation is present in certain time lags. We calculate RMSE to verify if the apparent correlation is significant. As we can see in Tab. I, values for WT media are very close to 0, indicating no significant correlation between past and present velocities, as original tracks are similar to predicted model. In $APC^{-/-}$ conditioned media, we can see that RMSE value is higher than in the previous case. Nonetheless, this value correspond to the 5% of the total ACF value, which suggests that the correlation in velocities might be small. Thus, we demonstrate that there is no significant correlation between past and present velocities.

IV. CONCLUSIONS

In this work, we have created a three-dimensional segmentation model capable of eliminating diffraction captured by the microscope. We have also demonstrated that immune cells migrating in $APC^{-/-}$ conditioned media, which represents our cancerous model, do not follow an APR walker model as expected from control model. Instead, immune cells migrating in this media present higher velocities and straighter paths when compared to WT conditioned media.

This project demonstrates that further research is needed in the modeling of immune cells' migration patterns in cancerous conditioned media, as current random walk models fail to predict movement in $APC^{-/-}$ conditioned media.

Acknowledgments

I would like to express my sincere gratitude to my advisor Dr. Jordi Comelles Pujadas and David Bartolomé Català for the guidance through this project. Additionally, I would like to thank my family and friends for their support.

[1] P. Wu, A. Giri, S.X. Sun, D. Wirtz, *Three-dimensional cell migration does not follow a random walk.*, Proc. Natl. Acad. Sci. U.S.A. 111 (11) 3949-3954.

[2] Stringer, C., Wang, T., Michaelos, M. et al. *Cellpose: a generalist algorithm for cellular segmentation.*, Nat Methods 18, 100–106 (2021).

[3] Schindelin, J., Arganda-Carreras, I., Frise, E. et al. *Fiji: an open-source platform for biological-image analysis.* Nat Methods 9, 676–682 (2012).

[4] Pachitariu, M., Stringer, C., *Cellpose 2.0: how to train your own model.*, Nat Methods 19, 1634–1641 (2022).

[5] Ershov, D., Phan, MS., Pylvänäinen, J.W. et al. *TrackMate 7: integrating state-of-the-art segmentation algorithms into tracking pipelines.* Nat Methods 19, 829–832 (2022).

[6] Jaqaman, K., Loerke, D., Mettlen, M. et al. *Robust single-particle tracking in live-cell time-lapse sequences.* Nat Methods 5, 695–702 (2008).

[7] Gómez-de-Mariscal E, Grobe H, Pylvänäinen JW, Xénard L, Henriques R, Tinevez J-Y, et al. *CellTracksColab is a platform that enables compilation, analysis, and exploration of cell tracking data.* PLoS Biol 22(8): e3002740 (2024).

[8] Wu, PH., Giri, A., Wirtz, D. *Statistical analysis of cell migration in 3D using the anisotropic persistent random walk model.* Nat Protoc 10, 517–527 (2015).

Estudi dels patrons de migració de cel·lules immunes en càncer

Author: Pau Canaleta Vicente
Facultat de Física, Universitat de Barcelona, Diagonal 645, 08028 Barcelona, Spain.

Advisor: Jordi Comelles Pujadas

Resum: La migració de les cèl·lules immunes és un procés de gran importància necessari per respondre a patògens que poden ser presents al nostre cos. Tot i que s'ha demostrat que la migració cel·lular en espais 3D segueix un model APRW, en aquest projecte demostrem que això no és cert per cèl·lules immunes migrant en un medi condicionat $APC^{-/-}$. Hem desenvolupat un model de segmentació d'imatges 3D per poder realitzar el seguiment de les cèl·lules. Amb el seguiment d'aquestes, hem demostrat que en aquest medi les cèl·lules immunes migren a velocitats més altes i amb camins més rectes, contrari al que és descrit pel model APRW.
Paraules clau: Caminant aleatori, Processament d'imatge, Analisis de trajectòries, Subdifusió
ODSs: ODS 3, ODS 15

Objectius de Desenvolupament Sostenible (ODSs o SDGs)

1. Fi de la es desigualtats		10. Reducció de les desigualtats	
2. Fam zero		11. Ciutats i comunitats sostenibles	
3. Salut i benestar	X	12. Consum i producció responsables	
4. Educació de qualitat		13. Acció climàtica	
5. Igualtat de gènere		14. Vida submarina	
6. Aigua neta i sanejament		15. Vida terrestre	X
7. Energia neta i sostenible		16. Pau, justícia i institucions sòlides	
8. Treball digne i creixement econòmic		17. Aliança pels objectius	
9. Indústria, innovació, infraestructures			